

Title	Insight into miscibility behaviour of cellulose ester blends with N-vinyl pyrrolidone copolymers in terms of viscometric interaction parameters
Author(s)	Sugimura, Kazuki; Teramoto, Yoshikuni; Nishio, Yoshiyuki
Citation	Cellulose (2015), 22(4): 2349-2363
Issue Date	2015-05-19
URL	<a href="http://hdl.handle.net/2433/201837">http://hdl.handle.net/2433/201837</a>
Right	The final publication is available at Springer via <a href="http://dx.doi.org/10.1007/s10570-015-0660-9">http://dx.doi.org/10.1007/s10570-015-0660-9</a> .; The full-text file will be made open to the public on 19 May 2016 in accordance with publisher's 'Terms and Conditions for Self-Archiving'.
Type	Journal Article
Textversion	author

1

2 **Insight into miscibility behaviour of cellulose ester blends with *N*-vinyl pyrrolidone**  
3 **copolymers in terms of viscometric interaction parameters**

4

5

6 Kazuki Sugimura, Yoshikuni Teramoto, and Yoshiyuki Nishio\*

7

8 *Division of Forest and Biomaterials Science, Graduate School of Agriculture, Kyoto*  
9 *University, Kyoto 606-8502, Japan*

10

11 \*To whom correspondence should be addressed.

12 E-mail: ynishio@kais.kyoto-u.ac.jp. Tel.: +81 75 753 6250. Fax: +81 75 753 6300.

13

14 **Abstract:** We previously offered miscibility maps for blend systems of cellulose esters  
15 (CEs) including cellulose acetate (CA), propionate (CP), and butyrate (CB) with vinyl  
16 copolymers containing an *N*-vinyl pyrrolidone (VP) unit, i.e., poly(*N*-vinyl  
17 pyrrolidone-*co*-vinyl acetate) (P(VP-*co*-VAc)) and poly(*N*-vinyl pyrrolidone-*co*-methyl  
18 methacrylate) (P(VP-*co*-MMA)); the maps were constructed based on data of thermal analysis  
19 as a function of the degree of ester substitution (DS) of the CE component and the VP fraction  
20 in the copolymer component. The blend system using CP among the three CEs imparted the  
21 largest region of miscible pairings with the vinyl copolymers, and both of the maps for the  
22 CP/P(VP-*co*-VAc) and CP/P(VP-*co*-MMA) systems comprised a "miscibility window"  
23 associated with the respective copolymer compositions at high DSs of >2.65. The present  
24 work was made to interpret the expansion of the miscible markings for the CP/copolymer  
25 systems in comparison with the cases using CA and CB, in terms of a Krigbaum-Wall  
26 interaction parameter ( $\mu$ ) obtained by solution viscometry for selective polymer pairs involved  
27 in the respective CE/copolymer blends. The results of  $\mu$  measurements were in good  
28 accordance with the earlier miscibility estimations. The assessment of very small negative  $\mu$   
29 values (i.e., extremely weak repulsion) for CP/PVAc and CP/PMMA combinations and that of  
30 considerably larger negative  $\mu$  values for PVP/PVAc and PVP/PMMA combinations enabled  
31 us to give a rational explanation for the CP systems. The strongly repellent character of the  
32 two different monomer units constituting the copolymers permits accession of the CP  
33 component (DS > 2.65) to them, which would be responsible for the advent of the miscibility  
34 window. Further expansion of the window observed when cellulose acetate propionate  
35 (CAP) was adopted instead of CP as the CE component was also well explained on the basis  
36 of a  $\mu$  data indicative of additional intramolecular repulsion in the CAP side.

37

38 **Keywords:** Blend miscibility; Cellulose ester; Interaction parameter; Miscibility window;  
39 *N*-Vinyl pyrrolidone

40

## 41 **Introduction**

42

43 Organic esters of cellulose (CEs) are commercially important polymers over nearly a century.  
44 They are widely prevailing in application fields such as coating, drug delivery (excipients),  
45 molded plastics including biodegradable ones, fibers, optical films, and membranes and other  
46 separation media (Edgar et al. 2001; Rustemeyer 2004). For improvement in physical  
47 properties of CEs toward their further applications, the designing of high-functional  
48 multicomponent materials based on the cellulose via graft copolymerization or polymer  
49 blending is a significant approach (Edgar et al. 2001; Nishio 2006; Yamaguchi 2010;  
50 Sugimura et al. in press). In the field of optical materials such as regulator or modulator of  
51 polarized light in modern displays, great attention of researchers has been focused on the  
52 delicate control of orientation birefringence and its wavelength dependence for CE-based  
53 films (Ohno and Nishio 2007a; Yamaguchi 2010; Yamaguchi et al. 2012; Yamanaka et al.  
54 2013; Sugimura et al. 2013b; Hayakawa and Ueda 2015; Sugimura et al. in press).  
55 Especially, miscible polymer blending is practically useful to manipulate the physical  
56 properties and functions of CEs readily at the lowest cost possible. Therefore, there have  
57 been a number of fundamental and practical blend studies of CEs; the counter components to  
58 CEs are categorized into mainly two sorts of polymers, biodegradable aliphatic polyesters  
59 such as poly(3-hydroxybutyrate) and poly( $\epsilon$ -caprolactone) (Nishio et al. 1997; Edgar et al.  
60 2001; Nishio 2006; Kusumi et al. 2008; Higeshiro et al. 2009), and synthetic vinyl polymers  
61 (Miyashita et al. 2002; Ohno et al. 2005; Nishio 2006; Ohno and Nishio 2006; Ohno and  
62 Nishio 2007a; Ohno and Nishio 2007b; Yamaguchi 2010; Yamaguchi et al. 2012; Yoshitake et  
63 al. 2013; Sugimura et al. 2013a; Sugimura et al. 2013b; Sugimura et al. in press).

64 Against the background stated above, the authors' group has recently performed basic  
65 characterization of miscibility and intermolecular interaction on binary blends of CEs with  
66 non-crystalline vinyl polymers, particularly poly(*N*-vinyl pyrrolidone) (PVP) and its random

67 copolymers (Miyashita et al. 2002; Ohno et al. 2005; Ohno and Nishio 2006; Ohno and  
68 Nishio 2007b; Sugimura et al. 2013a; Sugimura et al. 2013b). The CE component mainly  
69 used in the previous studies was cellulose acetate (CA), propionate (CP), or butyrate (CB)  
70 (Fig. 1a), and poly(*N*-vinyl pyrrolidone-*co*-vinyl acetate) (P(VP-*co*-VAc)) (Fig. 1b) or  
71 poly(*N*-vinyl pyrrolidone-*co*-methyl methacrylate) (P(VP-*co*-MMA)) (Fig. 1c) was the  
72 counter polymer component. Fig. 2a–c survey miscibility estimations for the blend systems  
73 of CA, CP, and CB, each combined with P(VP-*co*-VAc) (designated as CE/P(VP-*co*-VAc))  
74 (Miyashita et al. 2002; Ohno and Nishio 2006; Sugimura et al. 2013a), by offering the  
75 miscibility map constructed as a function of the degree of ester substitution (DS) of CE and  
76 the copolymer composition of P(VP-*co*-VAc). The mappings were made based on thermal  
77 analysis ( $T_g$  detection) by differential scanning calorimetry (DSC). As can readily be seen  
78 by comparison of the three maps, the miscibility behaviour of CE/P(VP-*co*-VAc) blends is  
79 seriously affected by a small difference in alkyl chain-length (carbon number) of the acyl  
80 substituent in the employed CE. The CP system produced the largest miscible region.

81 << **Figure 1 (a) & (b) & (c)** >>

82 << **Figure 2 (a) & (b) & (c)** >>

83 Similar representations of miscibility estimations are given in Fig. 3 for two systems in  
84 which P(VP-*co*-MMA) was combined with either CA (Ohno and Nishio 2007b) or CP  
85 (Sugimura et al. 2013b); however, the mapping for CB/P(VP-*co*-MMA) blends is not made in  
86 this figure (see later discussion). Again interestingly, the miscible pairing region for the  
87 CP/P(VP-*co*-MMA) system is much larger than that for the CA/P(VP-*co*-MMA) system, with  
88 spreading to the upper right side of higher DS of CP and lower VP fraction of  
89 P(VP-*co*-MMA) in the map.

90 << **Figure 3 (a) & (b)** >>

91 Using supplementary data from Fourier transform infrared (FT-IR) and solid-state NMR  
92 measurements, we have tentatively concluded that the CE/VP-containing copolymer

93 combinations assume miscible or immiscible behaviour according to the balance in  
94 effectiveness of the following four factors (Sugimura et al. 2013a; Sugimura et al. 2013b): (1)  
95 hydrogen-bonding attraction between residual hydroxyls of CE and VP-carbonyl groups of  
96 the vinyl (co)polymer; (2) steric hindrance of bulky side-groups to the interaction specified in  
97 (1); (3) indirect attraction via intramolecular repulsion between the comonomer units in the  
98 copolymer; and (4) weak interaction due to structural affinity (e.g., dipole-dipole antiparallel  
99 alignment) between the ester side-group of CE (such as CH<sub>3</sub>-CH<sub>2</sub>-CO-O-C-) and the VAc  
100 (-(CH<sub>2</sub>-CH(O-CO-CH<sub>3</sub>))-) or MMA (-(CH<sub>2</sub>-(CH<sub>3</sub>)C(-CO-O-CH<sub>3</sub>))-) unit. To explain the  
101 factor 3 more lucidly, when two monomer species having mutually repellent characters are  
102 randomly combined by covalent bonding, the copolymers tend to form a miscible phase with  
103 the CE component in the binary blends, rather than self-associate with the strong  
104 intramolecular repulsion. Unfortunately, however, the factors 3 and 4 could not be directly  
105 detected by the spectroscopic measurements.

106 In the present comparative study of the CE/vinyl polymer blends, we aim to clarify the  
107 contributions of the copolymer effect and structural affinity to the miscibility attainment, by  
108 another method besides thermal and spectroscopic techniques. In a previous work (Ohno  
109 and Nishio 2007b), we preliminarily estimated the attractive or repulsive action between  
110 chain segments of the polymer ingredients participating in the three systems,  
111 CA/P(VP-co-VAc), CA/P(VP-co-MMA), and CB/P(VP-co-VAc), in terms of Krigbaum-Wall  
112 polymer-polymer interaction parameters ( $\Delta b$  and  $\mu$ ) determinable by dilute solution  
113 viscometry. Particularly  $\mu$  data gave a satisfactory account of the difference in the  
114 miscibility behaviour between the three blend systems (see later discussion). In this context,  
115 the present paper covers complementary assessments of  $\mu$  parameters for various ingredient  
116 polymer pairs involved with the CP/P(VP-co-VAc) and CP/P(VP-co-MMA) systems.  
117 Through comprehensive comparison of the results with the  $\mu$  data formerly obtained for the  
118 CA and CB systems, some profound insights are provided into the positive effect of propionyl

119 substitution leading to expansion of the miscible paring region in the maps of the CP systems.  
120 Additional attention is turned to miscibility behaviour of CB/P(VP-*co*-MMA) and cellulose  
121 acetate propionate (CAP)/P(VP-*co*-MMA) blends.

122

## 123 **Experimental**

124

### 125 **Materials**

126

127 CA was kindly provided from Daicel Corporation, and CAP was purchased from Eastman  
128 Chemical Co. CP and CB samples were synthesized with acid chloride/base catalyst from  
129 cotton cellulose via a homogeneous reaction in our laboratory, as has been described in the  
130 preceding papers (Nishio et al. 1997; Ohno and Nishio 2006; Kusumi et al. 2008). Table 1  
131 summarizes the characterization data including DS, molecular weight, and glass transition  
132 temperature ( $T_g$ ) determined by DSC (see below) for all the CE samples used in this study.  
133 Codes "CE<sub>x</sub>" and "CA<sub>y</sub>P<sub>z</sub>" denote CE of ester DS =  $x$  and CAP of acetyl DS =  $y$  and propionyl  
134 DS =  $z$ , respectively.

135

### << **Table 1** >>

136 The vinyl polymers employed as a mixing partner for the CEs were PVP, PVAc,  
137 poly(methyl methacrylate) (PMMA), P(VP-*co*-VAc), and P(VP-*co*-MMA). Data of  
138 characterization for all the vinyl polymers are also listed in Table 1. As shown in the table,  
139 any of the copolymer samples exhibited a single  $T_g$ , and the  $T_g$ -copolymer composition  
140 relationships were in good obedience to a well-known Fox equation (Fox and Flory 1954),  
141 with a possible extent of scattering due to the difference in molecular weight; thus they were  
142 all regarded as essentially random copolymer. Hereafter, a P(VP-*co*-VAc) copolymer of  
143 VP:VAc =  $m:n$  (in molar ratio) is encoded as P(VP <sub>$m$</sub> -*co*-VAc <sub>$n$</sub> ), and the same encoding rule is  
144 also applied for P(VP-*co*-MMA) samples.

145

146 Preparation of blend samples

147

148 Powder materials of CEs and vinyl polymers were individually dissolved in  
149 *N,N*-dimethylformamide (DMF) at room temperature (~25 °C), at a polymer concentration of  
150 1.00 g dL<sup>-1</sup>. Blend solutions for viscometric measurements were prepared by mixing equal  
151 amounts of two solutions of the component polymers. For DSC measurements, two  
152 solutions of the required pairing polymers were mixed at the desired weight proportions.  
153 The mixed polymer solutions (transparent) were then poured into a Teflon<sup>®</sup> tray and film  
154 samples were made by evaporation of DMF at 50 °C under reduced pressure (< 10 mmHg).  
155 The as-cast films were further dried at 50 °C *in vacuo* for 3 days, before supplying to the  
156 thermal analysis.

157

158 Measurements

159

160 Viscosity measurements were performed for dilute polymer solutions in DMF with an  
161 Ubbelohde capillary viscometer, which was placed in a thermo-regulated water bath (30 °C).  
162 The temperature of the water bath was controlled within an accuracy range of ±0.1 °C. The  
163 polymer concentration of the starting sample was adjusted to 1.00 g dL<sup>-1</sup>, and dilutions of the  
164 solutions were made to yield at least 4 lower concentrations by adding appropriate doses of  
165 DMF. The measurements following the respective dilutions were done after elapsing of an  
166 equilibrium time of 15 min. As for the polymer solutions containing CP<sub>2.72</sub> or CB<sub>2.67</sub>,  
167 however, the viscometric data were actually collected in a polymer concentration range below  
168 ~0.30 g dL<sup>-1</sup>, because the solutions of 1.00 g dL<sup>-1</sup> were appreciably viscous due to  
169 comparatively high molecular weights of the cellulosics (see Table 1). The elution time of  
170 each solution from the set gauge of the viscometer was determined as the average of five



171 readings.

172 DSC thermal analysis was carried out with a Seiko DSC 6200/EXSTAR 6000 apparatus.  
173 The temperature readings were calibrated with an indium standard. The calorimetry  
174 measurements were conducted on ca. 5-mg film samples packed in an aluminum pan under a  
175 nitrogen atmosphere. Each sample was first heated from ambient temperature (~25 °C) to  
176 ~220 °C at a scanning rate of 20 °C min<sup>-1</sup>, and then immediately quenched to -50 °C at a rate  
177 of 80 °C min<sup>-1</sup>. Following this, the second heating scan was run from -50 °C to 230 °C at a  
178 rate of 20 °C min<sup>-1</sup> to record stable thermograms. Thermograms presented in this paper  
179 were all obtained in the second heating scan, and the  $T_g$  was taken as a temperature at the  
180 midpoint of a baseline shift in heat flow characterizing the glass transition.

181

## 182 **Results and discussion**

183

### 184 Quantification of interaction parameters

185

186 Following the preceding work (Ohno and Nishio 2007b), we applied a viscometric method  
187 developed by Krigbaum and Wall (Krigbaum and Wall 1950) and other groups (Cragg and  
188 Bigelow 1955; Chee 1990), to assess the attractive or repulsive interactivity between the  
189 CE-vinyl polymer constituents focused so far in this series of blend studies. The result was  
190 greatly useful to understand the difference in miscibility behaviour between the blend systems,  
191 as embodied in a later discussion.

192 A viscometric interaction parameter,  $b$ , for a non-electrolyte dilute polymer solution  
193 (usually, in the concentration range lower than ~1.0 g dL<sup>-1</sup>) is defined to fulfill a linear  
194 relationship given by the Huggins equation (Huggins 1942):

$$195 \quad \eta_{sp}/c = [\eta] + bc \quad (1)$$

196 where  $c$  is the solute concentration, and  $\eta_{sp}$  and  $[\eta]$  are the so-called specific and intrinsic

197 viscosities, respectively. The  $b$  is assumed to reflect an interaction between chain molecules  
 198 of the considered polymer and determined from a slope of the plot of  $\eta_{sp}/c$  vs.  $c$ . The  
 199 parameter  $b$  is also related to the Huggins coefficient  $k$  by

$$200 \quad b = k[\eta]^2 \quad (2)$$

201 The  $k$  value generally ranges from 0.3 (in good solvents) to  $\sim 0.7$  (in the  $\Theta$  state) (Bohdanecký  
 202 and Kovář 1982).

203 With regard to a blend solution of two different polymers in a common solvent, Equation  
 204 (1) is applicable in a rewritten fashion:

$$205 \quad (\eta_{sp})_m / c_m = [\eta]_m + b_m c_m \quad (3)$$

206 where the subscript  $m$  denotes "mixture", and  $b_m$  is a comprehensive viscometric interaction  
 207 parameter that reflects an overall interaction involving three possible combinations of  
 208 polymer chains of the same species (1-1 and 2-2) or not (1-2).

209 In this viscometric treatment, the polymer-polymer miscibility is estimated by  
 210 comparison between an experimentally obtained value and an ideally calculated one of  $b_m$ .  
 211 The former value,  $b_m^{ex}$ , is determined from the plot of  $(\eta_{sp})_m / c_m$  vs.  $c_m$  for blend solutions of a  
 212 given polymer pair. The latter ideal value,  $b_m^{id}$ , is calculated by the following equation  
 213 (Krigbaum and Wall 1950):

$$214 \quad b_m^{id} = w_1^2 b_{11} + w_2^2 b_{22} + 2w_1 w_2 b_{12} \quad (4)$$

215 where  $w_i$  is the weight fraction of component  $i$  in the polymer mixture, and  $b_{ij}$  is an interaction  
 216 parameter between the molecular chain of polymer  $i$  and that of polymer  $j$ , and thereby a  
 217 potential value of  $b_{12}$  may be given by

$$218 \quad b_{12} = \sqrt{b_{11} \times b_{22}} \quad (5)$$

219 Here, a Krigbaum-Wall interaction parameter,  $\Delta b$ , is defined as

$$220 \quad \Delta b = b_m^{ex} - b_m^{id} \quad (6)$$

221 If  $\Delta b$  is positive, the polymer 1 and polymer 2 are mutually attractive and therefore the pair is  
 222 taken as miscible. Contrarily, if  $\Delta b$  is negative, the repulsive pair is considered to be

223 immiscible. When there is a large difference between  $[\eta]$  values of both polymers ( $[\eta]_1$  and  
224  $[\eta]_2$ ), the following alternative parameter  $\mu$  as a standard in non-dimensional unit may be  
225 more useful to predict the miscibility between the two components (Chee 1990).

$$226 \quad \mu = \frac{\Delta b}{([\eta]_2 - [\eta]_1)^2} \quad (7)$$

227 The absolute value of  $\mu$ , i.e.,  $|\mu|$ , should represent the relative strength of attractive or  
228 repulsive interaction between the two component polymer molecules.

229 Table 2 summarizes data of  $[\eta]$  and  $b$  parameters ( $b_m^{\text{ex}}$  and  $b_m^{\text{id}}$ ) obtained by the  
230 viscometry for DMF solutions of CEs, vinyl polymers, and selected blending pairs of 50/50  
231 composition, together with the polymer-polymer interaction parameters  $\Delta b$  and  $\mu$  determined  
232 for the blends. The values of  $[\eta]$  and  $b_m^{\text{ex}}$  were obtained directly from the reduced viscosity  
233 ( $\eta_{\text{sp}}/c$ ) versus concentration plots, and those of  $b_m^{\text{id}}$ ,  $\Delta b$ , and  $\mu$  were calculated by the relevant  
234 equations ((4), (6), and (7)) given above. For comprehensive purposes, some data were  
235 quoted from the previous paper (Ohno and Nishio 2007b). As can be seen in the table, the  
236  $[\eta]$  values of the cellulosics and those of the vinyl (co)polymers are fairly far apart, and hence  
237 the standardized parameter  $\mu$  is mainly used below for discussion on the interaction and  
238 miscibility between the blend constituents.

239 << **Table 2** >>

240

241 Overview of  $\mu$  records for CA and CB blends

242

243 First, we briefly review the preceding results of  $\mu$  assessment for CA/P(VP-co-VAc),  
244 CB/P(VP-co-VAc), and CA/P(VP-co-MMA) blends (Ohno and Nishio 2007b). Figs. 4a, 4c,  
245 and 5a summarize simplified miscibility maps of the three blend systems, with addition of the  
246 illustrations in terms of  $\mu$  data obtained for selected polymer combinations (DS of CEs, ~2.7;  
247 VP:VAc or MMA of copolymers, ~0.5:0.5) critical to the respective systems. The individual  
248  $\mu$  evaluations were in consistency with the respective miscibility mappings based on DSC

249 thermal analysis; viz., a positive  $\mu$  value was obtained for miscible pairs of  
250 cellulosic/synthetic polymers, while immiscible blends all provided a negative  $\mu$  value.

251 << **Figure 4 (a) & (b) & (c)** >>

252 << **Figure 5 (a) & (b)** >>

253 As exemplified for a highly butyrate CB/P(VP-*co*-VAc) series (Fig. 4c, right), the  $\mu$  data  
254 concerned with the "three" constituting polymer ingredients made an order with respect to  
255 the degree of "immiscibility": PVP/PVAc ( $-4.23 \times 10^{-2}$ ) > CB<sub>2.67</sub>/PVP ( $-1.43 \times 10^{-2}$ )  $\geq$   
256 CB<sub>2.67</sub>/PVAc ( $-1.07 \times 10^{-2}$ ). The mutually repellent character of the PVP/PVAc pair is  
257 considerably stronger than the corresponding ones of the other pairs CB<sub>2.67</sub>/PVP and  
258 CB<sub>2.67</sub>/PVAc. Then it can be taken for the CB<sub>2.67</sub>/P(VP<sub>0.52</sub>-*co*-VAc<sub>0.48</sub>) blend that the  
259 P(VP-*co*-VAc) component was intimately mixed with the CB component showing less  
260 repulsion to both the comonomer units, as a result of avoidance of the intense repulsion  
261 between VP and VAc segments inevitable in the copolymer-copolymer association; the  
262 blending pair of CB<sub>2.67</sub>/P(VP<sub>0.52</sub>-*co*-VAc<sub>0.48</sub>) is surely attractive to each other, giving a positive  
263  $\mu$  value,  $+3.69 \times 10^{-3}$ . This reasoning would satisfy us about the appearance of the miscibility  
264 window (Fig. 4c, left), as amplified in the following sections. On the other hand, such an  
265 explicit window never appeared in the map of the CA/P(VP-*co*-VAc) system (see Fig. 2a and  
266 4a), although there should have arisen the intra-copolymer effect improving the miscibility in  
267 the blends of relatively high-acetylated CAs. The absence of the window may be interpreted  
268 as due to an inhibiting factor, i.e., the strong self-association ability of highly substituted CAs  
269 of DS > 2.7; the CAs are rather easily crystallizable as cellulose triacetate II form. Differing  
270 from this, no crystallizing habit was detected even for a CB synthesized at DS = 2.94 (Ohno  
271 and Nishio 2006). The lesser self-association nature of CB should be advantageous to that  
272 attractive interaction with the P(VP-*co*-VAc) component.

273 Meanwhile, another vinyl polymer combination of PVP and PMMA provided a  $\mu$  value  
274 of  $-1.87 \times 10^{-2}$ , from which the binary system is suggested to be immiscible. In fact, the

275 blend samples showed a common behaviour of essentially double  $T_g$ s in DSC measurements  
276 (Ohno and Nishio 2007b). However, the  $|\mu|$  value for the PVP/PMMA pair is smaller than  
277 that ( $|\mu| = 4.23 \times 10^{-2}$ ) for the PVP/PVAc pair. Thus it is deduced that the constituents VP and  
278 MMA in P(VP-co-MMA) show a somewhat weaker repulsive interaction than the VP and  
279 VAc units in P(VP-co-VAc). Presumably, this deterioration of the latent copolymer effect is  
280 responsible for the observation of a narrower miscible region in the CA/P(VP-co-MMA) map  
281 (Fig. 5a) relative to that in the CA/P(VP-co-VAc) map (Fig. 4a).

282

283 Inspection of miscibility maps for CP blends in  $\mu$  terms

284

285 *CP/P(VP-co-VAc) system*

286 As shown in Fig. 4b (right), a negative  $\mu$  value  $-1.02 \times 10^{-2}$  was obtained for the combination  
287 of CP<sub>2.72</sub> and PVP homopolymer, while  $\mu$  of the CP<sub>2.72</sub>/P(VP<sub>0.52</sub>-co-VAc<sub>0.48</sub>) pair was positive,  
288  $+1.50 \times 10^{-2}$ . From these assessments, PVP and P(VP<sub>0.52</sub>-co-VAc<sub>0.48</sub>) are taken as immiscible  
289 and miscible, respectively, with the highly esterified CP. The judgment is actually in  
290 accordance with the result of miscibility estimation by thermal analysis for the blends (see Fig.  
291 4b, left). For another essential pair, CP<sub>2.72</sub>/PVAc, we obtained a negative  $\mu$  of  $-7.19 \times 10^{-5}$ ,  
292 but the absolute value is much smaller than that for the CP<sub>2.72</sub>/PVP pair by more than two  
293 orders of magnitude. The former pair was previously marked to be partially miscible by  
294 observation of two  $T_g$ s approaching each other to an appreciable extent, and the low  
295 magnitude of  $\mu$  reflects such a "better compatibility" of highly substituted CP with PVAc  
296 homopolymer.

297 Despite no presence of strong intermolecular attraction between CP<sub>2.72</sub> and the two  
298 homopolymers (PVP and PVAc), the CP component was able to be miscible with the  
299 copolymer comprising VP and VAc units. This phenomenon is explicable as being due to  
300 the more intense repulsive action between the VP and VAc segments in the P(VP-co-VAc)

301 copolymer component, as in the case of the CB/P(VP-*co*-VAc) system. We find for sure in  
302 Fig. 4b (right) that the PVP/PVAc pair shows the largest negative  $\mu$  value ( $-4.23 \times 10^{-2}$ ) in the  
303 three polymer pairs participating in the CP<sub>2.72</sub>/P(VP-*co*-VAc) system. In general, when two  
304 monomer species repelling each other are randomly combined by covalent bonding, the  
305 resulting copolymer tends to intimately mix with the other polymer of less self-associating  
306 nature, so as to reduce the strong repulsion between the comonomer units (ten Brinke et al.  
307 1983; Paul and Barlow 1984). This is the reason why the high-esterified CP and CB can be  
308 miscible with P(VP-*co*-VAc) in a restricted range of the copolymer composition, even though  
309 there is a scarcity of specific attractive force (i.e. proton donor-acceptor interaction) between  
310 the two mixing components.

311 As is obvious in Fig. 4, the miscible region in the CP/P(VP-*co*-VAc) map is larger than  
312 the corresponding ones in the other maps of CA/P(VP-*co*-VAc) and CB/P(VP-*co*-VAc). In  
313 perspective comparison, the region involved in the CP system expands particularly to the side  
314 of VAc-rich compositions. This improvement virtually comes from the better  
315 compatibility of CP with PVAc supported above by the  $\mu$  data of  $-7.19 \times 10^{-5}$  for CP<sub>2.72</sub>/PVAc.  
316 This value in  $|\mu|$  is overwhelmingly small, compared with  $\mu = -2.12 \times 10^{-2}$  for CA<sub>2.70</sub>/PVAc  
317 (Fig. 4a, right) and  $\mu = -1.07 \times 10^{-2}$  for CB<sub>2.67</sub>/PVAc (Fig. 4c, right).

318 For three pairs of P(VP<sub>0.52-*co*}-VAc<sub>0.48</sub>) with the CEs of DS  $\approx$  2.7, we can rank them  
319 according to  $\mu$  data, as follows: CA<sub>2.70</sub>/P(VP<sub>0.52-*co*}-VAc<sub>0.48</sub>) ( $+7.12 \times 10^{-2}$ ) >  
320 CP<sub>2.72</sub>/P(VP<sub>0.52-*co*}-VAc<sub>0.48</sub>) ( $+1.50 \times 10^{-2}$ ) > CB<sub>2.67</sub>/P(VP<sub>0.52-*co*}-VAc<sub>0.48</sub>) ( $+3.69 \times 10^{-3}$ ), all  
321 showing miscibility. The CA<sub>2.70</sub>/P(VP<sub>0.52-*co*}-VAc<sub>0.48</sub>) pair exhibited the highest  $\mu$  value,  
322 which is attributable to the direct interaction based on the actually detected hydrogen bonding  
323 between CA-hydroxyl and VP-carbonyl groups (Miyashita et al. 2002; Ohno et al. 2005);  
324 however, the increase of  $\mu$  relative to that for CA<sub>2.70</sub>/PVP ( $+4.53 \times 10^{-2}$ ) suggests a secondary  
325 contribution of the intra-copolymer effect to the miscibility attainment. The hydrogen  
326 bonding effect seriously declines in the other two systems adopting propionyl and butyryl</sub></sub></sub></sub></sub>

327 substitutions for the CE component. Consequently, the miscibility of CB<sub>2.67</sub> with  
328 P(VP<sub>0.52-co</sub>-VAc<sub>0.48</sub>) is realized only through the intra-copolymer repulsion as an indirect  
329 driving force. As to the CP<sub>2.72</sub>/P(VP<sub>0.52-co</sub>-VAc<sub>0.48</sub>) pair, besides the copolymer effect, a  
330 weak interaction due to structural affinity between the propionyl ester group and VAc unit  
331 also acts as a factor contributory to the miscibility attainment.

332

333 *CP/P(VP-co-MMA) system*

334 Fig. 5b (left) displays a simplified diagram of the miscibility mapping conducted for  
335 CP/P(VP-co-MMA) blends (Fig. 3b). In the right side of Fig. 5b,  $\mu$  data are collected for  
336 four combinations of CP<sub>2.72</sub> with P(VP<sub>0.50-co</sub>-MMA<sub>0.50</sub>), P(VP<sub>0.22-co</sub>-MMA<sub>0.78</sub>), PVP, and  
337 PMMA, the values being  $+9.33 \times 10^{-4}$ ,  $+4.27 \times 10^{-3}$ ,  $-1.02 \times 10^{-2}$ , and  $-3.23 \times 10^{-4}$ , respectively.  
338 Judging from the positive or negative sign of  $\mu$ , the P(VP-co-MMA) copolymers are taken as  
339 potentially miscible with CP<sub>2.72</sub>, whereas both the homopolymers are not. These judgments  
340 entirely agree with the actual markings for the CP<sub>2.72</sub>/P(VP-co-MMA) series in the miscibility  
341 map. In addition, PVP/PMMA blends are immiscible and this polymer pair provides a larger  
342 negative  $\mu$  ( $-1.87 \times 10^{-2}$ ) than the CP<sub>2.72</sub>/PVP and CP<sub>2.72</sub>/PMMA pairs. The relationship in  
343 repulsion (immiscibility) between the three ingredient polymer pairs participating in the  
344 CP<sub>2.72</sub>/P(VP-co-MMA) series is basically similar to that found for the CP<sub>2.72</sub>/P(VP-co-VAc)  
345 series (see Fig. 4b, right). Accordingly, it is reasonable to assume that the intramolecular  
346 repulsive effect of the VP-MMA copolymer gave rise to the miscibility window in the map for  
347 the CP/P(VP-co-MMA) system. However, the window region observed for this system is  
348 obviously narrower than that for the CP/P(VP-co-VAc) system (see Fig. 4b, left). This  
349 narrowing of the window may be ascribed to the weaker repulsion in the VP-MMA  
350 copolymer relative to that in the VP-VAc copolymer ( $\mu = -4.23 \times 10^{-2}$ ), as has been applied to  
351 the comparative discussion of the two maps for the corresponding blends of CA. The  
352 location of the window in the side of MMA-rich compositions owes to the better affinity

353 between CP and MMA segments, as supported by the lower order ( $10^{-4}$ ) of  $\mu$  obtained for the  
354 CP<sub>2.72</sub>/PMMA pair.

355

356 Complementary mapping for CB/P(VP-*co*-MMA) system by application of  $\mu$  assessment

357

358 In the miscibility characterization of CE/vinyl copolymer blends, we have not yet  
359 accomplished the total mapping for the CB/P(VP-*co*-MMA) system by thermal analysis. A  
360 main reason is that  $T_g$ s (ca. 110–120 °C) of CBs of DS  $\approx$  2.5–2.9 are fairly close to those (ca.  
361 100–115 °C) of P(VP-*co*-MMA)s of VP < 50 mol%. However, we previously acquired the  
362 following data for the system concerned: (i) CB and PVP homopolymer formed miscible  
363 blends of hydrogen-bonding type unless the butyryl DS exceeded  $\sim$ 2.5 (see Fig. 2c) (Ohno  
364 and Nishio 2006); (ii) a polymer pair of CB (DS = 2.94) with P(VP<sub>0.50</sub>-*co*-MMA<sub>0.50</sub>) was  
365 judged to be immiscible (double  $T_g$ s) (Ohno and Nishio 2007b).

366 To depict the miscibility map of the CB/P(VP-*co*-MMA) system more closely, we newly  
367 examined the blend miscibility of relatively low-substituted CBs (DS < 2.5) with  
368 P(VP-*co*-MMA)s by DSC and also quantified  $\mu$  for additional pairs of CB (DS  $\geq$  2.6) with  
369 MMA-rich P(VP-*co*-MMA)s by viscometry. A major concern is whether the miscibility  
370 window emerges or not in the CB/P(VP-*co*-MMA) map.

371 Fig. 6a illustrates DSC thermograms measured for blend samples of CB<sub>2.01</sub>/PMMA  
372 homopolymer; the binary cast films were mostly cloudy to the naked eye. As can be seen  
373 from the data, two independent glass transitions originating from the two components were  
374 detected for the 40/60–80/20 compositions (in wt% ratio), signaling immiscibility of the  
375 CB<sub>2.01</sub>/PMMA pair. The same behaviour of double  $T_g$ s was also observed for CB<sub>2.41</sub>/PMMA  
376 blends. In contrast, Fig. 6b and c offer a typical miscible evidence in DSC (i.e.  
377 composition-dependent single  $T_g$ ) for CB<sub>2.01</sub>/P(VP<sub>0.22</sub>-*co*-MMA<sub>0.78</sub>) and  
378 CB<sub>2.01</sub>/P(VP<sub>0.50</sub>-*co*-MMA<sub>0.50</sub>) blends, respectively. Similar miscible behaviour was



379 confirmed for other polymer combinations using CB<sub>2.41</sub> and/or P(VP-*co*-MMA)s of VP  $\geq$  9  
380 mol% (MMA  $\leq$  91 mol%). Additionally, as-cast films of the CB blends with the  
381 P(VP-*co*-MMA)s were all highly transparent in the visual inspection. Thus it turns out that  
382 the lower limit in VP fraction of P(VP-*co*-MMA) that can be miscible with CB (DS  $<$   $\sim$ 2.5) is  
383  $\sim$ 10 mol%, which is almost the same limit as that found when CP was the CE component (see  
384 Fig. 5b). In a reasoning similar to that applied to interpret the CP/P(VP-*co*-MMA) map, the  
385 miscibility of CB with P(VP-*co*-MMA)s so rich in MMA residues (e.g. MMA = 87 and 91  
386 mol%) would be invited by a good compatibility between the butyl ester side-group and the  
387 MMA unit. This may be supported by  $\mu$  assessment of an extremely small negative value  
388 ( $-8.35 \times 10^{-5}$ ) for a polymer pair CB<sub>2.67</sub>/PMMA (see Table 2).

389 << **Figure 6 (a) & (b) & (c)** >>

390 In the present viscometric  $\mu$  measurements, we found a definitely positive data such as  $\mu$   
391  $= +2.12 \times 10^{-3}$  for CB<sub>2.67</sub>/P(VP<sub>0.22</sub>-*co*-MMA<sub>0.78</sub>). This indicates that even CB of DS  $>$  2.5 is  
392 potentially miscible with the vinyl copolymer rich in MMA. Fig. 7 (left) summarizes a  
393 miscibility map constructed for the total system of CB/P(VP-*co*-MMA) by the combined use  
394 of the DSC and  $\mu$ -assessment results. In the map, solid lines separate the miscible and  
395 immiscible regions connected with DS of CB and VP fraction of P(VP-*co*-MMA), to provide a  
396 miscibility window in the upper right portion. As illustrated in the right side in Fig. 7,  $\mu$   
397 parameters for three combinations of the ingredient polymers pertinent to the  
398 CB<sub>2.67</sub>/P(VP-*co*-MMA) series are all negative, but the PVP/PMMA pair gives the largest  
399 absolute value ( $1.87 \times 10^{-2}$ ). This situation again supports the contribution of the  
400 intramolecular repulsion inherent in the P(VP-*co*-MMA) copolymer to the appearance of the  
401 miscibility window. However, the region is diminished to some extent, compared to the  
402 window in the CB/P(VP-*co*-VAc) map (Fig. 4c), because the repulsion between VP and MMA  
403 units is weaker than that between VP and VAc units, as already mentioned above.

404 << **Figure 7** >>

405 Here we should further note that CB<sub>2.67</sub> of DS  $\approx$  2.7 is estimated to be immiscible with  
406 P(VP<sub>0.50-co</sub>-MMA<sub>0.50</sub>) of VP:MMA = 50:50 from the  $\mu$  data of  $-3.39 \times 10^{-3}$ . In contrast, a  
407 comparable pair using CP, i.e., CP<sub>2.72</sub>/P(VP<sub>0.50-co</sub>-MMA<sub>0.50</sub>), was miscible, which was  
408 decisive from both  $T_g$  and  $\mu$  determinations (see Figs. 3b and 5b). It follows, therefore, that  
409 the miscible pairing region (mainly associated with the window) in the CB/P(VP-co-MMA)  
410 map is a little narrower than that of the CP/P(VP-co-MMA) map. This comparison is made  
411 clearer in Fig. 7 (left), as guided by solid lines and broken ones inserted therein.

412 As indicated above, intimate mixing of two polymer components through the copolymer  
413 repulsion effect is unrealized on blending CB<sub>2.67</sub> with P(VP<sub>0.50-co</sub>-MMA<sub>0.50</sub>). In  
414 interpretation of this, the following data should be recalled:  $\mu = -1.87 \times 10^{-2}$  for PVP/PMMA  
415 and  $-1.43 \times 10^{-2}$  for CB<sub>2.67</sub>/PVP (see Fig. 7, right), the two values being close to each other.  
416 In the employment of the copolymer of VP = 50 mol%, probably, the relatively strong  
417 repulsion would still work between the CB component and the VP residue and inhibit the  
418 mutual approach of the two polymer components. Consequently, the intramolecular  
419 copolymer effect to attain miscible CB/P(VP-co-MMA) blends is active only at restricted  
420 copolymer compositions considerably rich in MMA. On the other hand, the repulsion  
421 between CP<sub>2.72</sub> and PVP ( $\mu = -1.02 \times 10^{-2}$ ) is evidently weaker than that between PVP and  
422 PMMA (see Fig. 5b, right), and the copolymer effect would be significant even at the  
423 composition of VP = 50 mol%, resulting in the miscible blending of the  
424 CP<sub>2.72</sub>/P(VP<sub>0.50-co</sub>-MMA<sub>0.50</sub>) pair. In addition, a low frequency of intermolecular  
425 hydrogen-bondings might contribute to this miscibility attainment as a secondary effect.  
426 This inference took into consideration the DS boundary of  $\sim$ 2.7 partitioning the mixing states  
427 of CP/P(VP-co-MMA) blends (VP  $\geq$  60 mol%) (Fig. 5b, left).

428

429 Inspection of estimation results of miscibility for CAP/P(VP-co-MMA) blends in  $\mu$  terms

430

431 Finally, we refer to miscibility behaviour of CAP blends with P(VP-*co*-MMA). To make a  
432 comparison with the result for the CP<sub>2.72</sub>/P(VP-*co*-MMA) series, a partially acetylated  
433 cellulose propionate sample, CA<sub>0.16</sub>P<sub>2.52</sub> (acetyl DS = 0.16; propionyl DS = 2.52), was  
434 selected as the mixed ester component.

435 Fig. 8 (left) collects the miscibility data (Sugimura et al. 2013b) based on thermal  
436 analysis for the target CA<sub>0.16</sub>P<sub>2.52</sub>/P(VP-*co*-MMA) blends, together with the corresponding  
437 data in the uses of CP<sub>2.72</sub> and CA<sub>2.70</sub>. In the right side, an additional illustration is given in  
438 terms of  $\mu$  assessment. The combination of CA<sub>0.16</sub>P<sub>2.52</sub> and P(VP<sub>0.50</sub>-*co*-MMA<sub>0.50</sub>) imparted  
439 a positive  $\mu$  value of  $+5.79 \times 10^{-3}$ , while negative  $\mu$  data of  $-1.01 \times 10^{-2}$  and  $-2.08 \times 10^{-4}$  were  
440 assigned to CA<sub>0.16</sub>P<sub>2.52</sub>/PVP and CA<sub>0.16</sub>P<sub>2.52</sub>/PMMA pairs, respectively. Therefore, the  
441 P(VP<sub>0.50</sub>-*co*-MMA<sub>0.50</sub>) copolymer is potentially miscible with the mixed ester CA<sub>0.16</sub>P<sub>2.52</sub>,  
442 whereas both the homopolymers are not. These judgments are consistent with the results of  
443 miscibility estimation by DSC for the respective blends, also supporting that the  
444 CA<sub>0.16</sub>P<sub>2.52</sub>/P(VP-*co*-MMA) series offers a miscibility window, as did the blend series using  
445 CP<sub>2.72</sub>. Furthermore, the immiscible polymer pair of PVP/PMMA provides a larger negative  
446  $\mu$  ( $-1.87 \times 10^{-2}$ ) than the other immiscible pairs of CA<sub>0.16</sub>P<sub>2.52</sub>/PVP and CA<sub>0.16</sub>P<sub>2.52</sub>/PMMA.  
447 From this triangular relationship, the intramolecular repulsive effect of the VP-MMA  
448 copolymer may be regarded as being responsible for the emergence of the miscibility window  
449 in the map for the CAP/P(VP-*co*-MMA) blends.

450 << **Figure 8** >>

451 However, it is astonishing that the VP:MMA range involved in the window became more  
452 expanded in the CA<sub>0.16</sub>P<sub>2.52</sub>/P(VP-*co*-MMA) series, when compared with the situation in the  
453 CP<sub>2.72</sub>/P(VP-*co*-MMA) series. In order to explain this expansion, we directed attention to  
454 another intramolecular repulsive interaction that might have arisen in the mixed ester  
455 component *per se*. Thereupon, a cellulose ester pair CA<sub>2.70</sub>/CP<sub>2.72</sub> was explored by thermal  
456 analysis and viscometry for evaluations of the miscibility and interaction parameter; the

457 residual hydroxyl contents of the monoester derivatives (CA<sub>2.70</sub> and CP<sub>2.72</sub>) are equalized to  
458 that of CA<sub>0.16</sub>P<sub>2.52</sub>. DSC measurements confirmed that CA<sub>2.70</sub>/CP<sub>2.72</sub> blends exhibited dual  
459  $T_g$  signals corresponding to those of the two constituents at any blending proportion. The  
460 Krigbaum-Wall interaction parameter of this polymer pair was estimated to be negative, as  $\mu$   
461  $= -8.12 \times 10^{-3}$  (see Fig. 8, right), in conformity with the immiscible behaviour of the blends.  
462 The absolute value of this  $\mu$  is appreciably large, although it is below  $|\mu| = 1.87 \times 10^{-2}$  for the  
463 PVP/PMMA pair. The present result suggests that a relatively strong repulsive interactivity  
464 can work between the two cellulosic ester components.

465 In view of the above context, it is deduced that the cellulose mixed ester would also  
466 behave as a kind of copolymer dangling two different ester groups along the carbohydrate  
467 backbone; thus, the CAP/P(VP-*co*-MMA) blends are taken as a copolymer/copolymer system  
468 where the miscibility should be affected by the duplicated, intramolecular copolymer effect.  
469 The expansion of the window in the mapping of the CA<sub>0.16</sub>P<sub>2.52</sub>/P(VP-*co*-MMA) blends can  
470 be ascribed to such an additional repulsion effect originating in the CAP side.

471

## 472 **Conclusions**

473

474 The blend miscibility of CP with the VP-containing vinyl copolymers P(VP-*co*-VAc) and  
475 P(VP-*co*-MMA) is improved in respect of the miscible pairing number, compared with the  
476 cases using CA and CB. This behaviour was satisfactorily explained by comparing the  
477 attractive or repulsive interactivities between related polymer ingredients in terms of the  
478 Krigbaum-Wall interaction parameter  $\mu$  that was determined by solution viscometry.  
479 Especially, great contributions of both the intra-copolymer effect and the structural affinity  
480 effect to the miscibility attainment were made clear by the  $\mu$  assessments. The former effect  
481 is explicitly responsible for the miscibility window appearing in the maps constructed for the  
482 CP/vinyl copolymer systems, and this is also applicable to the maps for the CB systems.

483 The comparatively narrower window observed when the counter component to CP or CB was  
484 P(VP-*co*-MMA) is interpretable as due to the lesser strength in repulsion of the VP-MMA  
485 copolymer relative to that of the VP-VAc copolymer. The structural affinity effect is  
486 concretely connected with a good compatibility of the propionyl group of CP with the VAc or  
487 MMA unit of the partner copolymer in the CP-based two systems, and, in the employment of  
488 CB, this effect is active between the butyryl and MMA moieties in the CB/P(VP-*co*-MMA)  
489 system only.

490 Such a useful  $\mu$  measurement was also applied to the inspection of miscibility mapping  
491 for CAP blends with P(VP-*co*-MMA). The observed expansion of the miscibility window  
492 relative to that for the comparable CP blends was explicable in terms of the  $\mu$  data, which  
493 indicated additional repulsion in the side of the cellulose mixed ester component; therefore,  
494 the CAP/P(VP-*co*-MMA) blends should be taken as a copolymer/copolymer system where the  
495 duplicated copolymer effect works.

496 From a practical standpoint, the present results will be so useful for related researchers to  
497 expand the opportunities of material design based on the CE family including cellulose mixed  
498 esters. Delicate characterization and even prediction of the miscibility may be possible for  
499 many other series of CE/synthetic copolymer blends by examining the viscometric interaction  
500 parameters of the targeted constituent polymer pairs, in addition to the orthodox thermal and  
501 spectroscopic estimations.

502

### 503 **Acknowledgements**

504 This work was financed by a Grant-in-Aid for Research Activity Start-up (No. 25892017  
505 to KS) as well as by a Grant-in-Aid for Scientific Research (A) (No. 26252025 to YN) from  
506 the Japan Society for the Promotion of Science.

507

### 508 **Compliance with Ethical Standards**

509 The authors declare no conflict of interest.

510

511 **Reference**

512 Bohdanecký M, Kovář J (1982) Viscosity of Polymer Solutions. Elsevier, Amsterdam

513 Chee KK (1990) Determination of polymer-polymer miscibility by viscometry. Eur Polym J  
514 26:423–426.

515 Cragg LH, Bigelow CC (1955) The Viscosity Slope Constant  $k'$ —Ternary Systems:  
516 Polymer–Polymer–Solvent. J Polym Sci 16:177–191.

517 Edgar KJ, Buchanan CM, Debenham JS, Rundquist PA, Seiler BD, Shelton MC, Tindall D  
518 (2001) Advances in cellulose ester performance and application. Prog Polym Sci  
519 26:1605–1688.

520 Fox TG, Flory PJ (1954) The Glass Temperature and Related Properties of Polystyrene.  
521 Influence of Molecular Weight. J Polym Sci 14:315–319.

522 Hayakawa D, Ueda K (2015) Computational study to evaluate the birefringence of uniaxially  
523 oriented film of cellulose triacetate. Carbohydr Res 402:146–151.

524 Higeshiro T, Teramoto Y, Nishio Y (2009) Poly(vinyl pyrrolidone-*co*-vinyl  
525 acetate)-*graft*-poly( $\epsilon$ -caprolactone) as a Compatibilizer for Cellulose  
526 Acetate/Poly( $\epsilon$ -caprolactone) Blends. J Appl Polym Sci 113:2945–2954.

527 Huggins M (1942) The Viscosity of Dilute Solutions of Long-Chain Molecules. IV.  
528 Dependence on Concentration. J Am Chem Soc 64:2716–2718.

529 Krigbaum WR, Wall FT (1950) Viscosities of binary polymeric mixtures. J Polym Sci  
530 5:505–514.

531 Kusumi R, Inoue Y, Shirakawa M, Miyashita Y, Nishio Y (2008) Cellulose alkyl  
532 ester/poly( $\epsilon$ -caprolactone) blends: characterization of miscibility and crystallization  
533 behaviour. Cellulose 15:1–16.

534 Liu Y, Huglin MB, Davis TP (1994) Preparation and characterization of some liner

535 copolymers as precursors to thermoplastic hydrogels. *Eur Polym J* 30:457–463.

536 Miyashita Y, Suzuki T, Nishio Y (2002) Miscibility of cellulose acetate with vinyl polymers.  
537 *Cellulose* 9:215–223.

538 Nishio Y (2006) Material Functionalization of Cellulose and Related Polysaccharides via  
539 Diverse Microcompositions. *Adv Polym Sci* 205:97–151.

540 Nishio Y, Matsuda K, Miyashita Y, Kimura N, Suzuki H (1997) Blends of  
541 poly( $\epsilon$ -caprolactone) with cellulose alkyl esters: effect of the alkyl side-chain length and  
542 degree of substitution on miscibility. *Cellulose* 4:131–145.

543 Ohno T, Nishio Y (2006) Cellulose alkyl ester/vinyl polymer blends: effects of butyryl  
544 substitution and intramolecular copolymer composition on the miscibility. *Cellulose*  
545 13:245–259.

546 Ohno T, Nishio Y (2007a) Molecular Orientation and Optical Anisotropy in Drawn Films of  
547 Miscible Blends Composed of Cellulose Acetate and Poly(*N*-vinylpyrrolidone-*co*-methyl  
548 methacrylate). *Macromolecules* 40:3468–3476.

549 Ohno T, Nishio Y (2007b) Estimation of Miscibility and Interaction for Cellulose Acetate and  
550 Butyrate Blends with *N*-Vinylpyrrolidone Copolymers. *Macromol Chem Phys*  
551 208:622–634.

552 Ohno T, Yoshizawa S, Miyashita Y, Nishio Y (2005) Interaction and Scale of Mixing in  
553 Cellulose Acetate/Poly(*N*-vinyl Pyrrolidone-*co*-vinyl Acetate) Blends. *Cellulose*  
554 12:281–291.

555 Paul DR, Barlow JW (1984) A binary interaction model for miscibility of copolymers in  
556 blends. *Polymer* 25:487–494.

557 Rustemeyer P (ed) (2004) *Cellulose Acetates: Properties and Applications*. Wiley-VCH,  
558 Weinheim

559 Sugimura K, Katano S, Teramoto Y, Nishio Y (2013a) Cellulose propionate/poly(*N*-vinyl  
560 pyrrolidone-*co*-vinyl acetate) blends: dependence of the miscibility on propionyl DS and

561 copolymer composition. *Cellulose* 20:239–252.

562 Sugimura K, Teramoto Y, Nishio Y (2013b) Blend miscibility of cellulose propionate with  
563 poly(*N*-vinyl pyrrolidone-*co*-methyl methacrylate). *Carbohydr Polym* 98:532–541.

564 Sugimura K, Teramoto Y, Nishio Y. Cellulose Acetate. In: Kobayashi S, Müllen K (eds)  
565 Encyclopedia of Polymeric Nanomaterials. Springer, Berlin/Heidelberg, in press. doi:  
566 10.1007/978-3-642-36199-9\_328-1

567 ten Brinke G, Karasz FE, MacKnight WJ (1983) Phase Behavior in Copolymer Blends:  
568 Poly(2,6-dimethyl-1,4-phenylene oxide) and Halogen-Substituted Styrene Copolymers.  
569 *Macromolecules* 16:1827–1832.

570 Yamaguchi M (2010) Optical Properties of Cellulose Esters and Their Blends. In: Lejeune A,  
571 Deprez T (eds) *Cellulose: Structure and Properties, Derivatives, and Industrial Uses*.  
572 Nova Science Publishers, New York, pp 325–340

573 Yamaguchi M, Manaf MEA, Songsurang K, Nobukawa S (2012) Material design of  
574 retardation films with extraordinary wavelength dispersion of orientation birefringence: a  
575 review. *Cellulose* 19:601–613.

576 Yamanaka H, Teramoto Y, Nishio Y (2013) Orientation and Birefringence Compensation of  
577 Trunk and Graft Chains in Drawn Films of Cellulose Acetate-*graft*-PMMA Synthesized  
578 by ATRP. *Macromolecules* 46:3074–3083.

579 Yoshitake S, Suzuki T, Miyashita Y, Aoki D, Teramoto Y, Nishio Y (2013) Nanoincorporation  
580 of layered double hydroxides into a miscible blend system of cellulose acetate with  
581 poly(acryloyl morpholine). *Carbohydr Polym* 93:331–338.

582

583



584

585 **Figure Captions**

586

587 **Fig. 1** Structural formulae of (a) CEs (i.e., CA, CP, and CB), (b) P(VP-*co*-VAc), and (c)  
588 P(VP-*co*-MMA).

589

590 **Fig. 2** Miscibility maps for three blend systems (a) CA/P(VP-*co*-VAc) (Miyashita et al.  
591 2002), (b) CP/P(VP-*co*-VAc) (Sugimura et al. 2013a), and (c) CB/P(VP-*co*-VAc) (Ohno and  
592 Nishio 2006), depicted as a function of DS of CE and VP fraction of the copolymer in a  
593 rearranged fashion with additional data. Symbols indicate that a given pair of CE/vinyl  
594 polymer is miscible (○, single  $T_g$ ), immiscible (×, dual  $T_g$ s), or partially miscible (△, dual  
595  $T_g$ s approaching each other to an appreciable degree).

596

597 **Fig. 3** Miscibility maps for two blend systems (a) CA/P(VP-*co*-MMA) (Ohno and Nishio  
598 2007b) and (b) CP/P(VP-*co*-MMA) (Sugimura et al. 2013b), depicted as a function of DS of  
599 CE and VP fraction of the copolymer in a rearranged fashion with additional data. The  
600 meanings of two symbols ○ and × are the same as defined in Fig. 2.

601

602 **Fig. 4** Miscibility maps (left) with additional illustrations using  $\mu$  data (right) for (a)  
603 CA/P(VP-*co*-VAc), (b) CP/P(VP-*co*-VAc), and (c) CB/P(VP-*co*-VAc) systems. The meanings  
604 of three symbols ○, ×, and △ are the same as used in Fig. 2. The miscibility maps are  
605 represented in a simplified style retaining the essence of the data shown in Fig. 2.

606

607 **Fig. 5** Miscibility maps (left) with additional illustrations using  $\mu$  data (right) for (a)  
608 CA/P(VP-*co*-MMA) and (b) CP/P(VP-*co*-MMA) systems. The meanings of two symbols ○  
609 and × are the same as used in Fig. 2. The miscibility maps are represented in a simplified  
610 style retaining the essence of the data shown in Fig. 3.

611

612 **Fig. 6** DSC thermograms obtained for blends of CB<sub>2.01</sub> with (a) PMMA, (b)  
613 P(VP<sub>0.22-co</sub>-MMA<sub>0.78</sub>), and (c) P(VP<sub>0.50-co</sub>-MMA<sub>0.50</sub>). Arrows indicate a  $T_g$  position taken  
614 as the midpoint of a baseline shift in heat flow.

615

616 **Fig. 7** Miscibility map (left) and additional illustration (right) using  $\mu$  data for  
617 CB/P(VP-*co*-MMA) blends. The meanings of two symbols  $\circ$  and  $\times$  are the same as used in  
618 Fig. 2. Solid lines in the map represent a boundary partitioning the miscible and immiscible  
619 regions for the CB/P(VP-*co*-MMA) system, and, for comparison, the corresponding boundary  
620 for the CP/P(VP-*co*-MMA) system (Fig. 5b) is drawn by broken lines.

621

622 **Fig. 8** Mapping of miscibility data (Sugimura et al. 2013b) (left) and additional illustration in  
623  $\mu$  terms (right) for CA<sub>0.16</sub>P<sub>2.52</sub>/P(VP-*co*-MMA) blends. For comparison, miscibility data for  
624 the corresponding blends using CA<sub>2.07</sub> and CP<sub>2.72</sub> (see Fig. 3) are also mapped in the left figure.  
625 The meanings of two symbols  $\circ$  and  $\times$  are the same as used in Fig. 2.

626

627 -----

628 In addition to the eight figures, there are two tables. See annexed sheets.

629

630

Sample code <sup>a</sup>	$M_w^d$	$M_n^d$	$M_w/M_n^d$	$T_g/^\circ\text{C}$	Source
CP <sub>2.72</sub>	1,070,000	367,000	2.92	134	Synthesized
CA <sub>0.16</sub> P <sub>2.52</sub>	258,000	73,400	3.51	143	Eastman Chemical Co.
CA <sub>2.70</sub>	237,000	73,000	3.25	186	Daicel Co.
CB <sub>2.67</sub>	998,000	285,000	3.50	114	Synthesized
CB <sub>2.41</sub>	952,000	218,000	4.37	132	Synthesized
CB <sub>2.01</sub>	651,000	294,000	2.21	139	Synthesized

Sample code	$M_w^e$	$M_n^e$	$M_w/M_n^e$	$T_g/^\circ\text{C}$	Source
PVP	24,500 <sup>f</sup>	–	–	162	Nacalai Tesque, Inc.
PVAc	90,000 <sup>f</sup>	–	–	41	Polyscience, Inc.
P(VP <sub>0.52-co-VAc</sub> <sub>0.48</sub> ) <sup>b</sup>	28,000	5,120	5.47	89	Polyscience, Inc.
PMMA	88,400	35,000	2.53	100	Aldrich Chemical Co.
P(VP <sub>0.22-co-MMA</sub> <sub>0.78</sub> ) <sup>c</sup>	189,000	70,800	2.66	111	Synthesized <sup>g</sup>
P(VP <sub>0.50-co-MMA</sub> <sub>0.50</sub> ) <sup>c</sup>	184,000	61,300	3.00	119	Synthesized <sup>g</sup>

<sup>a</sup> The DS values were determined by <sup>1</sup>H NMR.

<sup>b</sup> The VP content was determined by <sup>1</sup>H NMR.

<sup>c</sup> The VP contents were determined by FT-IR in a way described by Liu et al. (1994).

<sup>d</sup> Determined by gel permeation chromatography (mobile phase, tetrahydrofuran at 40 °C) with polystyrene standards.

<sup>e</sup> Determined by gel permeation chromatography (mobile phase, 10 mM L<sup>-1</sup> lithium bromide/DMF at 40 °C) with polystyrene standards.

<sup>f</sup> Nominal value.

<sup>g</sup> Synthesized in the authors' laboratory by radical polymerization of two distilled monomers, VP (Nacalai Tesque, Inc.) and MMA (Nacalai Tesque, Inc.), in the same way as that described in a previous paper (Ohno and Nishio 2007b).

633 **Table 2** Data of intrinsic viscosity and interaction parameters estimated by viscometry for

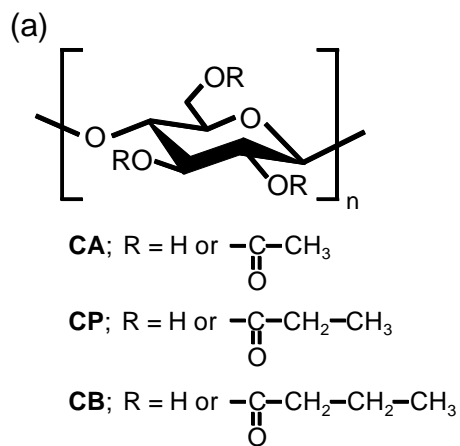
634 CEs, synthetic vinyl polymers, and their respective 50/50 blends

Samples	$[\eta]/\text{dL}\cdot\text{g}^{-1}$	$b_m^{\text{ex}}/\text{dL}^2\cdot\text{g}^{-2}$	$b_m^{\text{id}}/\text{dL}^2\cdot\text{g}^{-2}$	$\Delta b/\text{dL}^2\cdot\text{g}^{-2}$	$\mu$
CP <sub>2.72</sub>	6.27	1.84×10 <sup>1</sup>	–	–	–
CA <sub>0.16</sub> P <sub>2.52</sub>	1.85	1.84	–	–	–
CA <sub>2.70</sub> <sup>a</sup>	2.28	1.86	–	–	–
CB <sub>2.67</sub> <sup>a</sup>	5.61	1.13×10 <sup>1</sup>	–	–	–
PVP <sup>a</sup>	1.46×10 <sup>-1</sup>	1.18×10 <sup>-2</sup>	–	–	–
PVAc <sup>a</sup>	6.10×10 <sup>-1</sup>	1.32×10 <sup>-1</sup>	–	–	–
P(VP <sub>0.52-co</sub> -VAc <sub>0.48</sub> ) <sup>a</sup>	1.67×10 <sup>-1</sup>	1.21×10 <sup>-2</sup>	–	–	–
PMMA <sup>a</sup>	2.92×10 <sup>-1</sup>	3.01×10 <sup>-2</sup>	–	–	–
P(VP <sub>0.22-co</sub> -MMA <sub>0.78</sub> )	3.64×10 <sup>-1</sup>	3.45×10 <sup>-2</sup>	–	–	–
P(VP <sub>0.50-co</sub> -MMA <sub>0.50</sub> ) <sup>a</sup>	5.54×10 <sup>-1</sup>	9.47×10 <sup>-2</sup>	–	–	–
CP <sub>2.72</sub> /PVP	3.77	4.46	4.85	-3.84×10 <sup>-1</sup>	-1.02×10 <sup>-2</sup>
CP <sub>2.72</sub> /PVAc	3.42	5.42	5.42	-2.30×10 <sup>-3</sup>	-7.19×10 <sup>-5</sup>
CP <sub>2.72</sub> /P(VP <sub>0.52-co</sub> -VAc <sub>0.48</sub> )	3.20	5.41	4.85	+5.59×10 <sup>-1</sup>	+1.50×10 <sup>-2</sup>
CP <sub>2.72</sub> /PMMA	3.67	4.98	4.99	-1.15×10 <sup>-2</sup>	-3.23×10 <sup>-4</sup>
CP <sub>2.72</sub> /P(VP <sub>0.22-co</sub> -MMA <sub>0.78</sub> )	3.09	5.17	5.02	+1.49×10 <sup>-1</sup>	+4.27×10 <sup>-3</sup>
CP <sub>2.72</sub> /P(VP <sub>0.50-co</sub> -MMA <sub>0.50</sub> )	3.12	5.32	5.29	+3.05×10 <sup>-2</sup>	+9.33×10 <sup>-4</sup>
CA <sub>0.16</sub> P <sub>2.52</sub> /PVP	9.80×10 <sup>-1</sup>	5.06×10 <sup>-1</sup>	5.35×10 <sup>-1</sup>	-2.91×10 <sup>-2</sup>	-1.01×10 <sup>-2</sup>
CA <sub>0.16</sub> P <sub>2.52</sub> /PMMA	1.07	5.83×10 <sup>-1</sup>	5.84×10 <sup>-1</sup>	-5.03×10 <sup>-4</sup>	-2.08×10 <sup>-4</sup>
CA <sub>0.16</sub> P <sub>2.52</sub> /P(VP <sub>0.50-co</sub> -MMA <sub>0.50</sub> )	1.13	7.01×10 <sup>-1</sup>	6.91×10 <sup>-1</sup>	+9.71×10 <sup>-3</sup>	+5.79×10 <sup>-3</sup>
CA <sub>2.70</sub> /PVP <sup>a</sup>	1.38	7.50×10 <sup>-1</sup>	5.43×10 <sup>-1</sup>	+2.07×10 <sup>-1</sup>	+4.53×10 <sup>-2</sup>
CA <sub>2.70</sub> /PVAc <sup>a</sup>	1.47	6.87×10 <sup>-1</sup>	7.47×10 <sup>-1</sup>	-5.95×10 <sup>-2</sup>	-2.12×10 <sup>-2</sup>
CA <sub>2.70</sub> /P(VP <sub>0.52-co</sub> -VAc <sub>0.48</sub> ) <sup>a</sup>	1.61	8.63×10 <sup>-1</sup>	5.44×10 <sup>-1</sup>	+3.20×10 <sup>-1</sup>	+7.12×10 <sup>-2</sup>
CA <sub>2.70</sub> /PMMA <sup>a</sup>	1.28	5.85×10 <sup>-1</sup>	5.92×10 <sup>-1</sup>	-6.64×10 <sup>-3</sup>	-1.67×10 <sup>-3</sup>
CA <sub>2.70</sub> /P(VP <sub>0.50-co</sub> -MMA <sub>0.50</sub> ) <sup>a</sup>	1.40	6.78×10 <sup>-1</sup>	6.99×10 <sup>-1</sup>	-2.12×10 <sup>-2</sup>	-7.06×10 <sup>-3</sup>
CB <sub>2.67</sub> /PVP <sup>a</sup>	2.97	2.59	3.01	-4.27×10 <sup>-1</sup>	-1.43×10 <sup>-2</sup>
CB <sub>2.67</sub> /PVAc <sup>a</sup>	3.14	3.20	3.47	-2.69×10 <sup>-1</sup>	-1.07×10 <sup>-2</sup>
CB <sub>2.67</sub> /P(VP <sub>0.52-co</sub> -VAc <sub>0.48</sub> ) <sup>a</sup>	2.82	3.13	3.02	+1.10×10 <sup>-1</sup>	+3.69×10 <sup>-3</sup>
CB <sub>2.67</sub> /PMMA <sup>a</sup>	3.04	3.13	3.13	-2.37×10 <sup>-3</sup>	-8.35×10 <sup>-5</sup>
CB <sub>2.67</sub> /P(VP <sub>0.22-co</sub> -MMA <sub>0.78</sub> )	2.42	3.21	3.15	+5.84×10 <sup>-2</sup>	+2.12×10 <sup>-3</sup>
CB <sub>2.67</sub> /P(VP <sub>0.50-co</sub> -MMA <sub>0.50</sub> ) <sup>a</sup>	3.16	3.28	3.37	-8.67×10 <sup>-2</sup>	-3.39×10 <sup>-3</sup>
PVP/PVAc <sup>a</sup>	3.90×10 <sup>-1</sup>	4.66×10 <sup>-2</sup>	5.57×10 <sup>-2</sup>	-9.13×10 <sup>-3</sup>	-4.23×10 <sup>-2</sup>
PVP/PMMA	2.40×10 <sup>-1</sup>	1.95×10 <sup>-2</sup>	1.99×10 <sup>-2</sup>	-4.02×10 <sup>-4</sup>	-1.87×10 <sup>-2</sup>
CA <sub>2.70</sub> /CP <sub>2.72</sub>	4.34	7.88	8.01	-1.29×10 <sup>-1</sup>	-8.12×10 <sup>-3</sup>

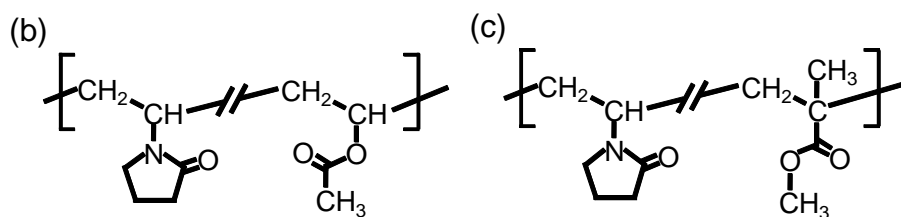
<sup>a</sup> Data were quoted from a previous paper (Ohno and Nishio 2007b).

635

636



637



638

639

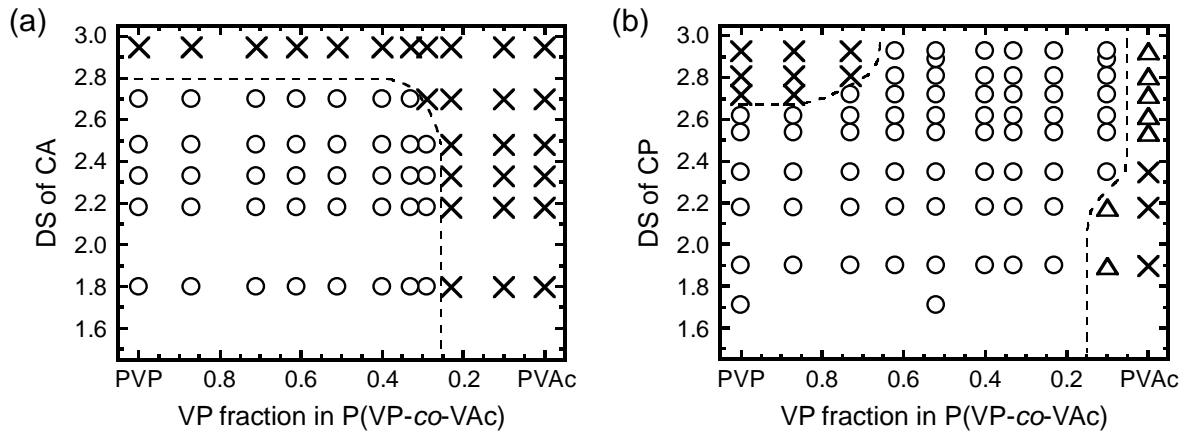
640 **Fig. 1** Structural formulae of (a) CEs (i.e., CA, CP, and CB), (b) P(VP-*co*-VAc), and (c)

641 P(VP-*co*-MMA).

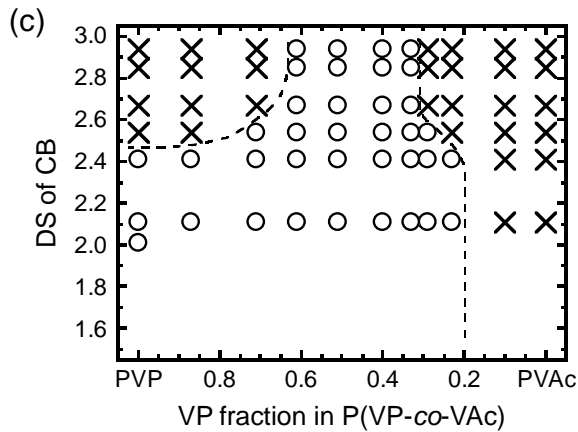
642

643

644



645



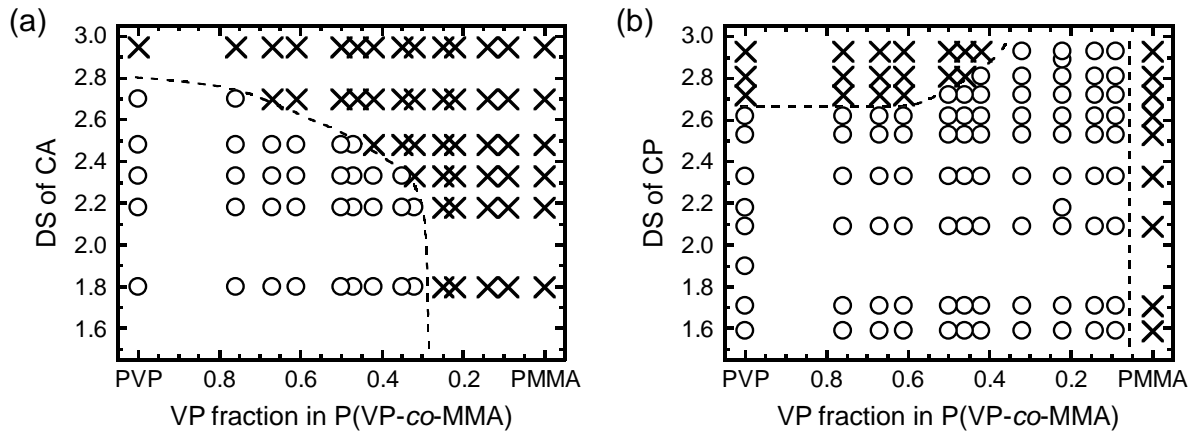
646

647

648 **Fig. 2** Miscibility maps for three blend systems (a) CA/P(VP-co-VAc) (Miyashita et al.  
649 2002), (b) CP/P(VP-co-VAc) (Sugimura et al. 2013a), and (c) CB/P(VP-co-VAc) (Ohno and  
650 Nishio 2006), depicted as a function of DS of CE and VP fraction of the copolymer in a  
651 rearranged fashion with additional data. Symbols indicate that a given pair of CE/vinyl  
652 polymer is miscible (○, single  $T_g$ ), immiscible (×, dual  $T_g$ s), or partially miscible (△, dual  
653  $T_g$ s approaching each other to an appreciable degree).

654

655



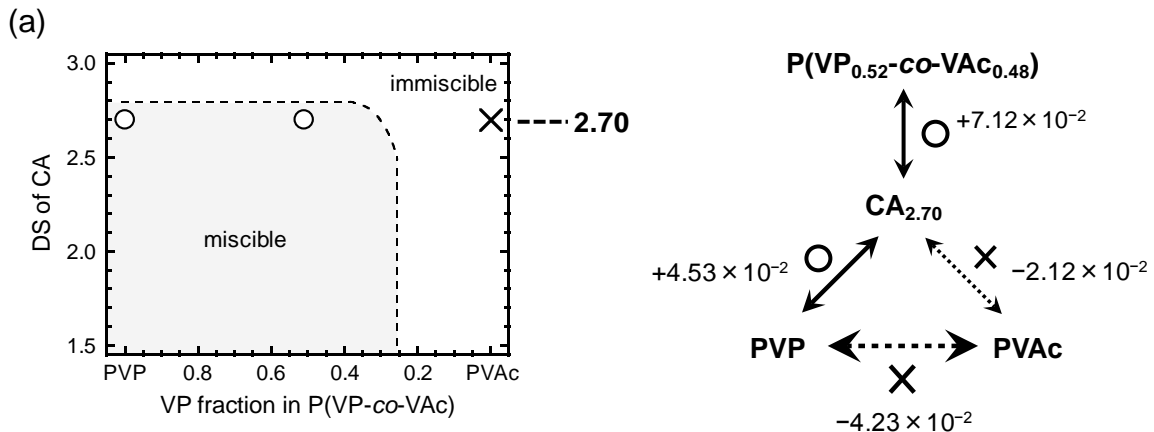
656

657

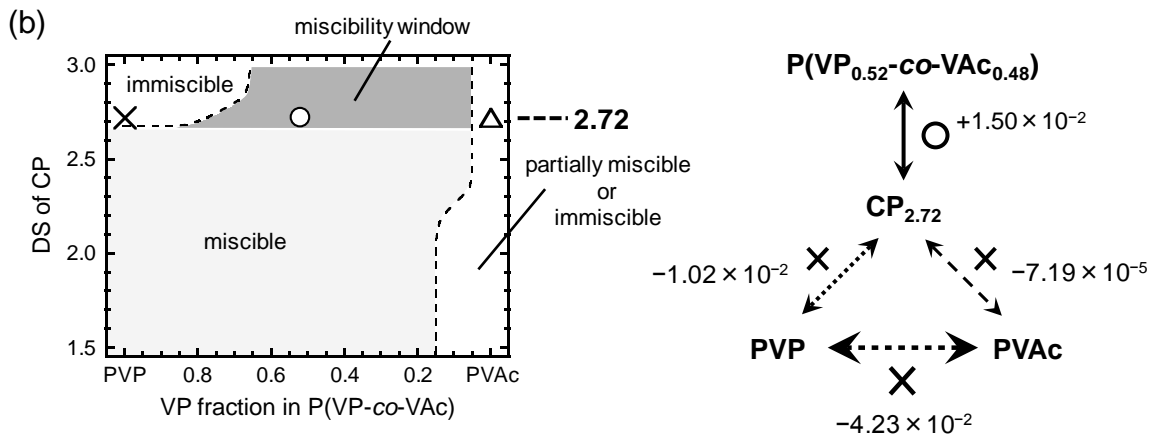
658 **Fig. 3** Miscibility maps for two blend systems (a) CA/P(VP-co-MMA) (Ohno and Nishio  
659 2007b) and (b) CP/P(VP-co-MMA) (Sugimura et al. 2013b), depicted as a function of DS of  
660 CE and VP fraction of the copolymer in a rearranged fashion with additional data. The  
661 meanings of two symbols ○ and × are the same as defined in Fig. 2.

662

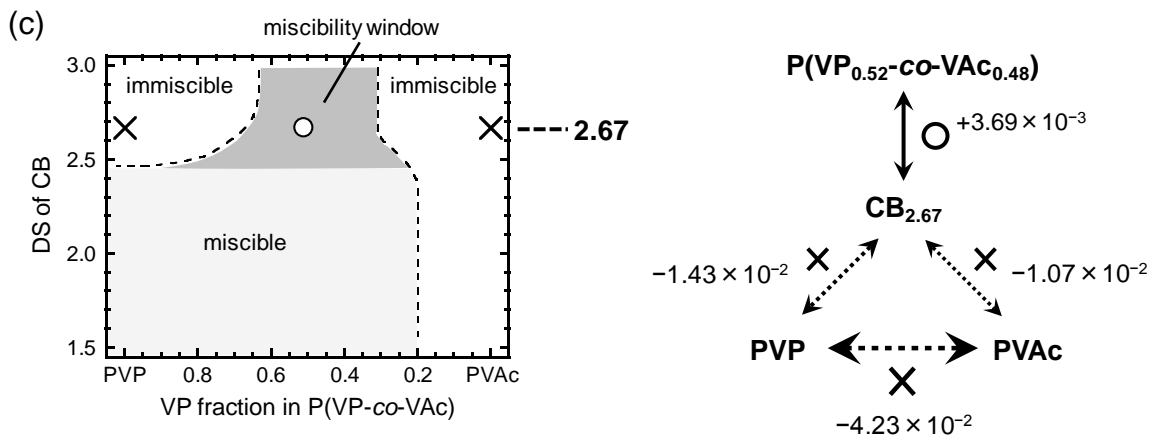
663



664



665



666

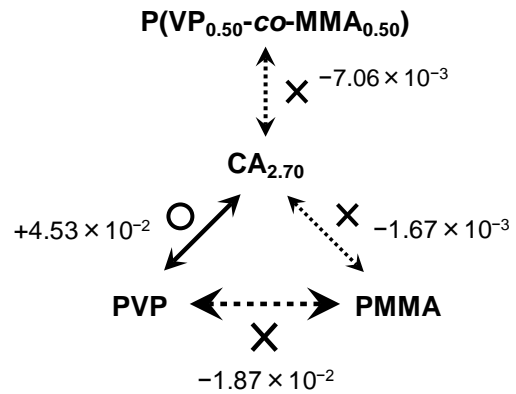
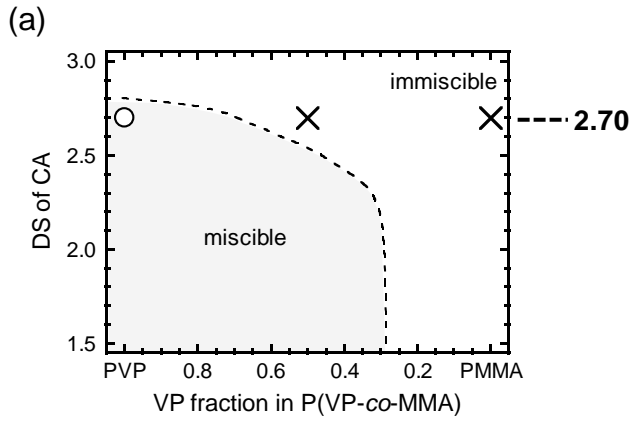
667

668 **Fig. 4** Miscibility maps (left) with additional illustrations using  $\mu$  data (right) for (a)  
 669 CA/P(VP-co-VAc), (b) CP/P(VP-co-VAc), and (c) CB/P(VP-co-VAc) systems. The meanings  
 670 of three symbols  $\circ$ ,  $\times$ , and  $\triangle$  are the same as used in Fig. 2. The miscibility maps are  
 671 represented in a simplified style retaining the essence of the data shown in Fig. 2.

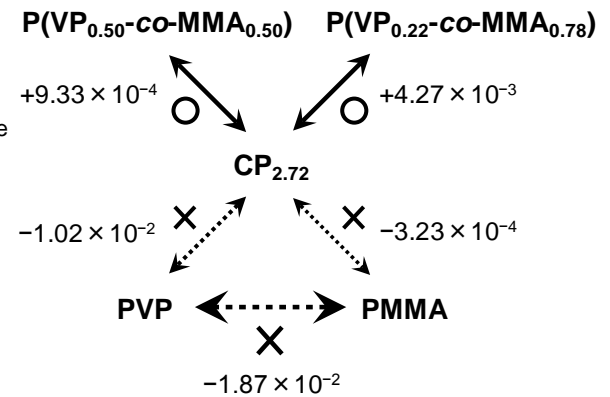
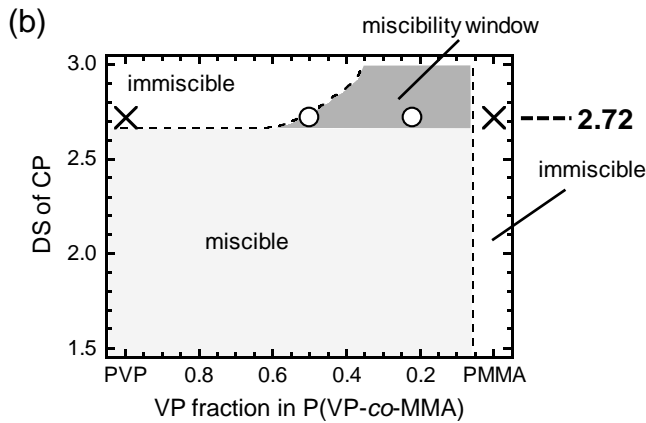
672



673



674



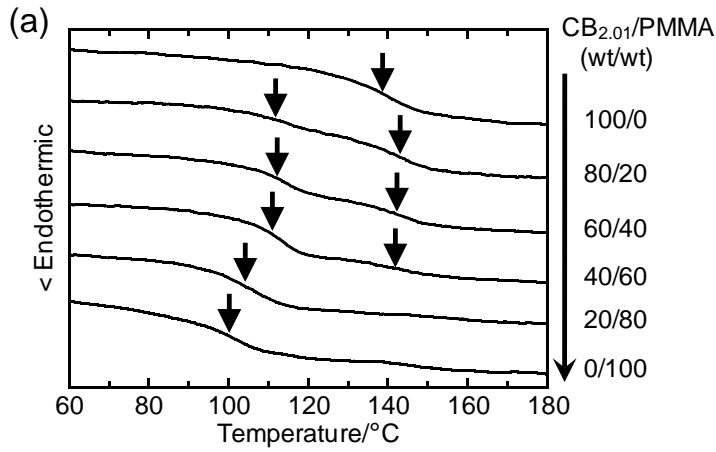
675

676

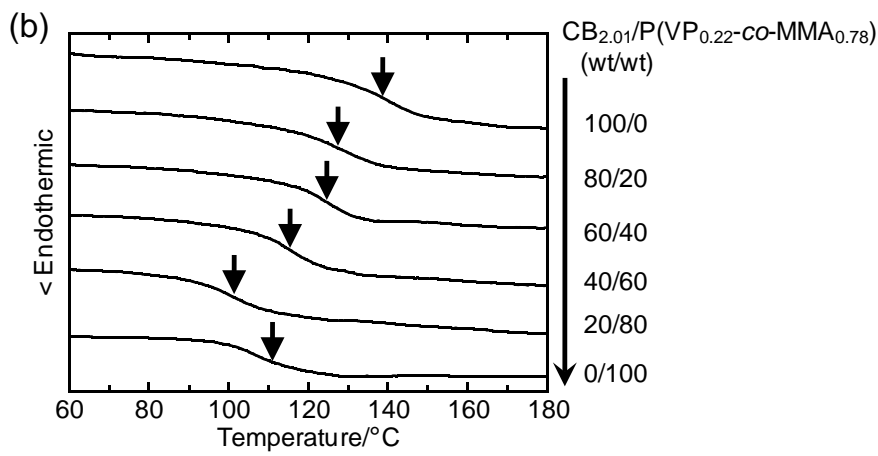
677 **Fig. 5** Miscibility maps (left) with additional illustrations using  $\mu$  data (right) for (a)  
 678 CA/P(VP-co-MMA) and (b) CP/P(VP-co-MMA) systems. The meanings of two symbols ○  
 679 and × are the same as used in Fig. 2. The miscibility maps are represented in a simplified  
 680 style retaining the essence of the data shown in Fig. 3.

681

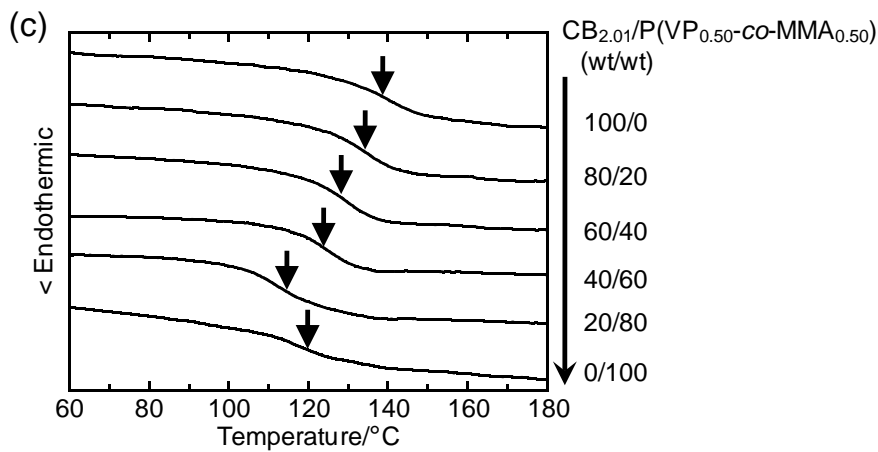
682



683



684



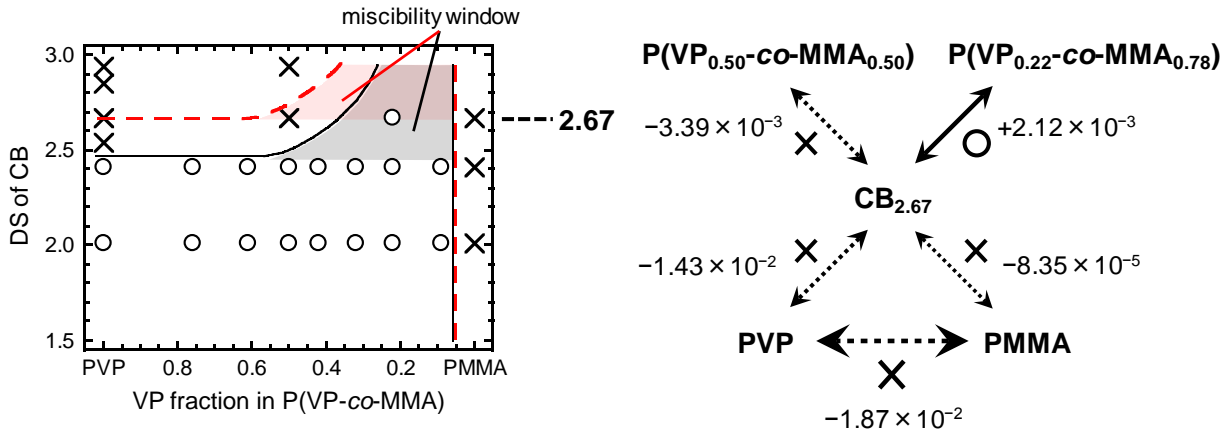
685

686

687 **Fig. 6** DSC thermograms obtained for blends of CB<sub>2.01</sub> with (a) PMMA, (b)  
688 P(VP<sub>0.22-co</sub>-MMA<sub>0.78</sub>), and (c) P(VP<sub>0.50-co</sub>-MMA<sub>0.50</sub>). Arrows indicate a T<sub>g</sub> position taken  
689 as the midpoint of a baseline shift in heat flow.

690

691



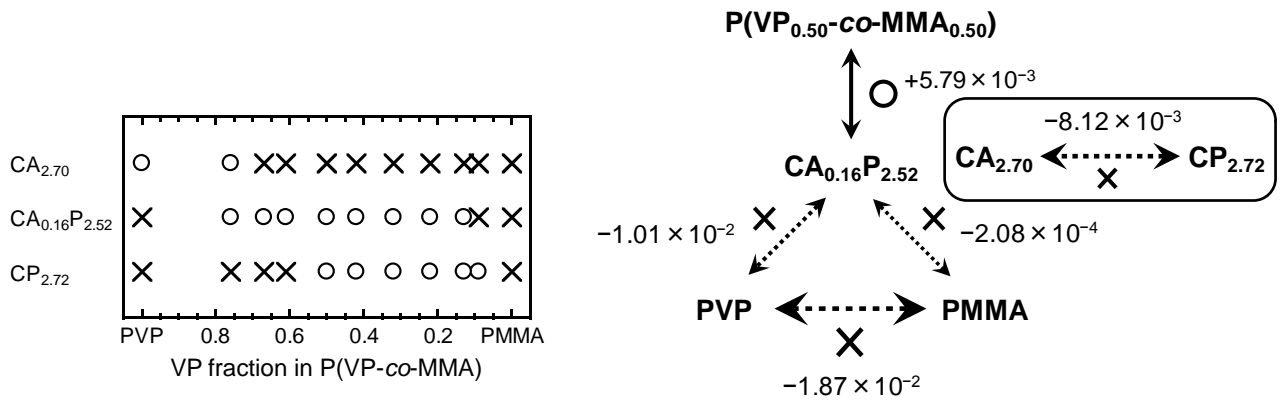
692

693

694 **Fig. 7** Miscibility map (left) and additional illustration (right) using  $\mu$  data for  
695 CB/P(VP-co-MMA) blends. The meanings of two symbols ○ and × are the same as used in  
696 Fig. 2. Solid lines in the map represent a boundary partitioning the miscible and immiscible  
697 regions for the CB/P(VP-co-MMA) system, and, for comparison, the corresponding boundary  
698 for the CP/P(VP-co-MMA) system (Fig. 5b) is drawn by broken lines.

699

700



701

702

703 **Fig. 8** Mapping of miscibility data (Sugimura et al. 2013b) (left) and additional illustration in  
 704  $\mu$  terms (right) for CA<sub>0.16</sub>P<sub>2.52</sub>/P(VP-co-MMA) blends. For comparison, miscibility data for  
 705 the corresponding blends using CA<sub>2.07</sub> and CP<sub>2.72</sub> (see Fig. 3) are also mapped in the left figure.  
 706 The meanings of two symbols ○ and × are the same as used in Fig. 2.

707